



The diacylglycerol kinase α (DGK α)/Akt/NF- κ B feedforward loop promotes esophageal squamous cell carcinoma (ESCC) progression via FAK-dependent and FAK-independent manner

Jie Chen¹ · Weimin Zhang¹ · Yan Wang¹ · Di Zhao¹ · Mengjiao Wu¹ · Jiawen Fan¹ · Jinting Li¹ · Ying Gong¹ · Nana Dan¹ · Di Yang¹ · Rui Liu¹ · Qimin Zhan^{1,2}

Received: 5 June 2018 / Revised: 29 October 2018 / Accepted: 13 November 2018
© Springer Nature Limited 2018

Abstract

Many reports have described DGK α as an oncogene, hence, we investigated its function and the underlying mechanisms in esophageal squamous cell carcinoma (ESCC) progression. This study demonstrated that DGK α was upregulated by inflammatory stimulants and formed feedforward loop with Akt/NF- κ B signaling in ESCC cells. Mechanistically, DGK α -activated Akt/NF- κ B signaling via stimulating PA production to reduce cAMP level and PTEN activity, and specifically, independently of its kinase function, through direct interaction with the FERM domain of FAK to relieve the auto-inhibitory effect of FERM domain on FAK. Overexpression of DGK α promoted cancer malignant progression both in vitro and in vivo, whereas depletion of DGK α suppressed these effects. Importantly, DGK α expression was tightly correlated with the malignancy of various inflammation-related squamous carcinomas and the oncogenic Akt/NF- κ B activity. Therefore, DGK α is critically involved in inflammation-mediated ESCC progression, supporting DGK α as a potential target for ESCC therapy.

Introduction

Chronic inflammation, induced by many risk factors including dietary factors, obesity, inhaled pollutants, alcohol consumption, and smoking, plays pivotal roles in the progression of cancers [1–3]. Mechanistically, inflammatory cells release proinflammatory mediators, such as tumor necrosis factor- α (TNF- α), interleukin-1 β , interleukin-6 (IL-1 β , IL-6), monocyte chemotactic protein-1 (MCP-1), and macrophage colony stimulating factor (GM-CSF), to directly stimulate oncogenic signaling in cancer cells,

including Akt/NF- κ B, HIF-1 α , and JAKs/STATs pathways [4, 5]. For example, lncRNA NMR functions as a mediator between NF- κ B pathway activation by cancer-related inflammatory cytokines (IL-1 β and TNF- α) and tumor progression in esophageal squamous cell carcinoma (ESCC) [6]. Regulation of FLOT1 expression effectively controls the TNF- α -activated IL-1 β and IL-6 in ESCC cells [7]. However, the molecular links of inflammatory cytokines and oncogenic signaling pathways in cancer cells remain largely unclear.

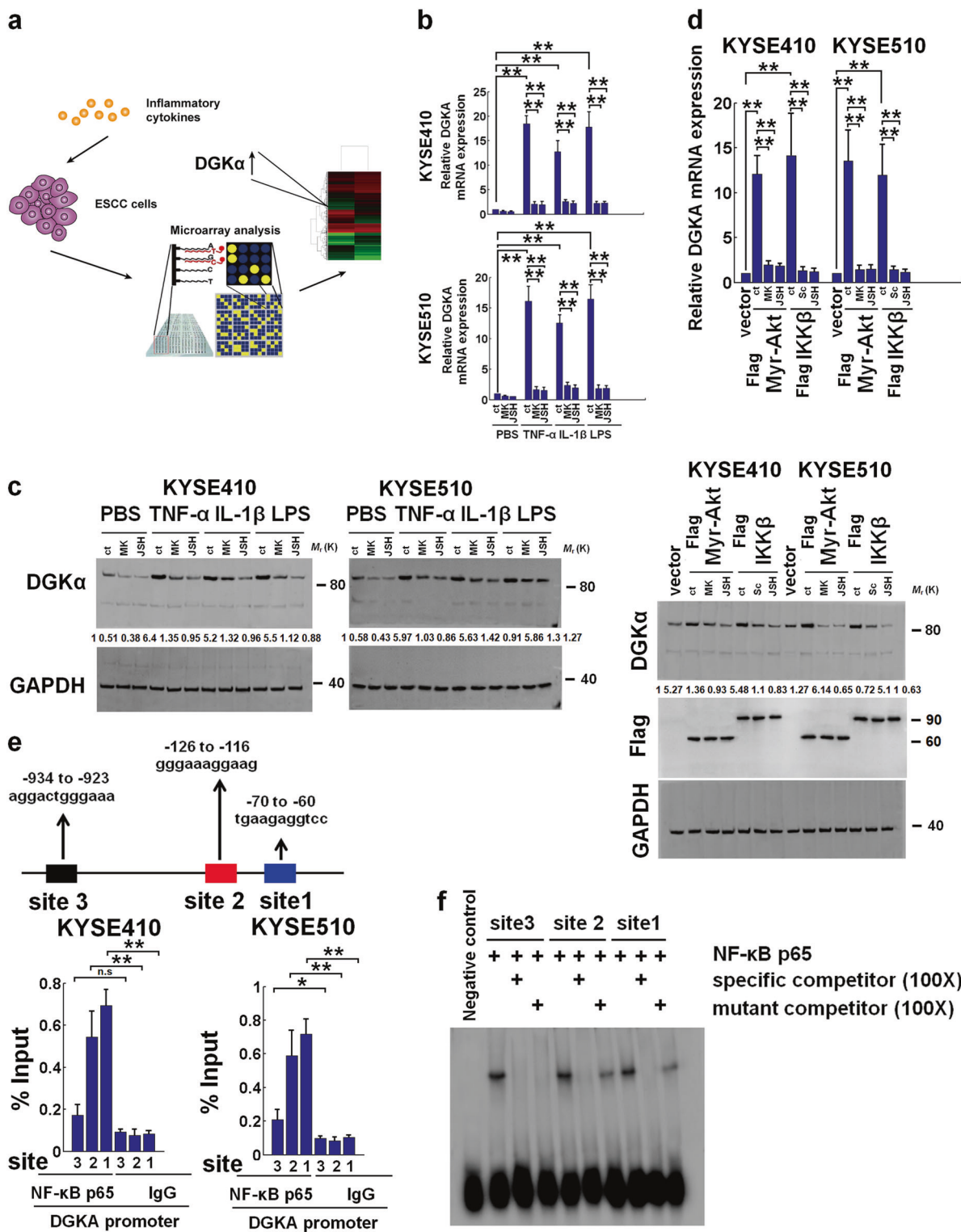
A series of studies have established the relationship between DGKs deregulation and inflammation [8]. Martinez et al. reported that inhibition of DGKs activity attenuates linoleic acid-mediated inflammation in human adipocytes [9]. DGK ζ , a type of DGKs, has been shown to interact with IQGAP1 and then to induce the phagocytosis in a lipopolysaccharide (LPS)-dependent manner in macrophages [10]. In addition to participating in inflammation, DGKs, especially DGK α , have also been shown to activate oncogenic signaling pathways and promote cancer progression. For example, DGK α activates Ras/Raf/MEK pathway to enhance hepatocellular carcinoma progression [11], interacts with Src to promote the growth of colon cancer cells [12], and produces PA to stimulate multiple oncogenic pathways to induce GBM progression [13]. Our

Supplementary material The online version of this article (<https://doi.org/10.1038/s41388-018-0604-6>) contains supplementary material, which is available to authorized users.

✉ Qimin Zhan
zhanqimin@bjmu.edu.cn

¹ Key laboratory of Carcinogenesis and Translational Research (Ministry of Education/Beijing), Laboratory of Molecular Oncology, Peking University Cancer Hospital & Institute, 100142 Beijing, China

² State Key Laboratory of Molecular Oncology, Cancer Institute and Cancer Hospital, Chinese Academy of Medical Sciences and Peking Union Medical College, Beijing 100021, China



systemic analyses identified that diacylglycerol kinase α (DGK α), a multisubstrate lipid kinase that catalyzes the production of phosphatidic acid (PA) from diacylglycerol, was significantly upregulated in response to various inflammatory stimulants in ESCC cells. However, the

biological functions of DGK α in ESCC progression remain elusive.

The aberrant activation of inflammation-related PI3K/Akt/NF- κ B pathway has been observed in many types of cancers [14–17]. The activation of PI3K/Akt is typically

◀ **Fig. 1** DGK α is upregulated by inflammatory cytokines via Akt/NF- κ B signaling. **a** Protocol of microarray assay. **b, c** Expression of DGK α assayed by real-time PCR (upper panel) (**b**) and immunoblotting (lower panel) (**c**) in KYSE410 or KYSE510 cells induced by inflammatory stimuli, including TNF- α (10 ng/ml), IL-1 β (10 ng/ml), or LPS (1 μ g/ml), or with or without Akt or NF- κ B inhibition by 10 μ M MK-2206 (MK) or 5 μ M JSH-23 (JSH). Expression levels were normalized to GAPDH. **d** Expression of DGK α assayed by real-time PCR (upper panel) and immunoblotting (lower panel) in KYSE410 or KYSE510 cells in the presence or absence of Flag-Myr-Akt or IKK β plasmid with or without Akt or NF- κ B inhibition by 10 μ M MK-2206, 5 μ M JSH-23, or 10 μ M Sc-3060 (Sc). Expression levels were normalized to GAPDH. **e** Analysis of the physical association of regions of the DGK α promoter with NF- κ B p65 by ChIP assays. Top, schematic illustration of PCR-amplified fragments of the DGK α promoter. Bottom, ChIP assays were performed in KYSE410 and KYSE510 cells. IgG served as the negative control. **f** Examination of NF- κ B p65 binding to different sites on the DGK α promoter using the EMSA assays. Purified protein NF- κ B p65 is incubated with biotin labeled ~30 base pair double stranded oligonucleotides spanning the predicted DGKA-binding sites at -934 to -923 (site 3), -126 to -116 (site 2), -70 to -60 (site 1) alone (the final concentration of oligonucleotide probe was 50 fmol), or in the presence of unlabeled respective competitor DNA or mutated (scrambled the core sequence) unlabeled competitor DNA in a 100-fold excess (the final concentration of 100-fold competitor was 5 pmol). n.s. no significant difference; * P < 0.05; ** P < 0.01; two-tailed unpaired Student's t -test. Error bars represent mean \pm SD of triplicate independent experiments

under the control of various kinases. Esther castellano et al. reported that the interaction of RAS with PI3K catalytic subunit-p110 α is required for the development of RAS-driven tumors [18]. Other studies reported that activated receptor tyrosine kinases, such as EGFR, PDGFR, and Her3, can interact with PI3K regulatory subunit-p85 and subsequently enhance the catalytic activity of PI3K [19, 20]. Furthermore, inhibition of TNF- α -induced truncated RXR α interaction with p85 can effectively suppress the activation of PI3K/Akt pathway and tumor growth in various tumors [21]. However, whether and how DGK α contributes to the activation of PI3K/Akt/NF- κ B pathway in ESCC cells remain to be illuminated. In this study, we aimed to investigate the contributions of DGK α in inflammatory cytokines-activated Akt/NF- κ B signaling in ESCC cells and its roles in the progression of ESCC.

Results

DGK α is upregulated by inflammatory cytokines via Akt/NF- κ B signaling

Dysregulated Akt/NF- κ B signaling promotes the progression of many cancers including ESCC [14–17]. Inflammatory cytokines, especially TNF- α and IL-1 β , stimulate Akt/NF- κ B signaling in cancer cells, especially ESCC [22–25]. Microarray assay was used to detect transcriptional profiles of KYSE410 ESCC cells treated by these cytokines and the

NF- κ B activator-LPS. The results showed that the expression of 102 genes was markedly increased, while the expression of 58 genes was significantly decreased more than two-fold under the stimulation of TNF- α , IL-1 β , and LPS. Specifically, DGK α was consistently elevated more than 13-fold by above inflammatory stimulants (Supplementary Table 1 and Fig. 1a). Real-time PCR and immunoblotting assays identified that DGK α expression was substantially promoted by above stimulants in KYSE410 and KYSE510 cells (Fig. 1b, c).

Then, whether Akt/NF- κ B signaling contributed to such induced DGK α expression was evaluated. MK-2206 (an inhibitor for Akt activation) and JSH-23 (an inhibitor for NF- κ B nuclear translocation), blocked the DGK α expression in KYSE410 and KYSE510 cells treated with inflammatory stimulants (Fig. 1b, c). Flag-tagged Akt (Myr-Akt) or IKK β (CA-IKK2) plasmid was transfected into KYSE410 and KYSE510 cells to induce Akt or NF- κ B activation and upregulate DGK α expression, which could be significantly suppressed by MK-2206, JSH-23, and Sc-3060 (another NF- κ B nuclear translocation inhibitor) (Fig. 1d). The existence of three NF- κ B-binding sites in the DGK α promoter region (site 1: 5'-TGAAGAGGTCC-3', -70 to -60; site 2: 5'-GGGAAAGGAAG-3', -126 to -116, and site 3: 5'-AGGACTGGGAAA-3', -934 to -923; https://www.ncbi.nlm.nih.gov/nucore/NM_001345.4) was identified by chromatin immunoprecipitation (ChIP) assay with anti-p65 antibody and electrophoretic mobility shift assay (EMSA) assay (Fig. 1e, f, Supplementary Fig. 2). The results of EMSA assay showed that MK-2206 and JSH23 blocked inflammatory cytokines-induced NF- κ B transcriptional activity (Supplementary Fig. 1a), and NF- κ B-DGK α promoter-binding activity (Supplementary Fig. 1b). Furthermore, MK-2206, JSH-23, and Sc-3060 inhibited NF- κ B activity (Supplementary Fig. 1c), and NF- κ B-DGK α promoter binding in ESCC cells harboring Flag-Myr-Akt or CA-IKK2 plasmid (Supplementary Fig. 1d).

DGK α positively regulates Akt/NF- κ B signaling

The relationship between DGK α expression and Akt/NF- κ B activity was assessed in 11 ESCC cell lines, two primary ESCC cells and two normal esophageal epithelial cells (NEECs). Figure 2a and Supplementary Figure 3 shows that the levels of DGK α were higher in indicated ESCC cell lines and primary ESCC cells than those in NEECs, and tightly associated with Akt/NF- κ B activity. Stable DGK α expression in ESCC cells increased Akt/NF- κ B activity, while stably silencing DGK α decreased it (Fig. 2b). Furthermore, TNF- α -induced Akt/NF- κ B activity was dramatically reduced in DGK α -silenced cells and strengthened in DGK α -overexpressed KYSE410 and KYSE510 cells (Fig. 2c). Additionally, depletion of DGK α substantially

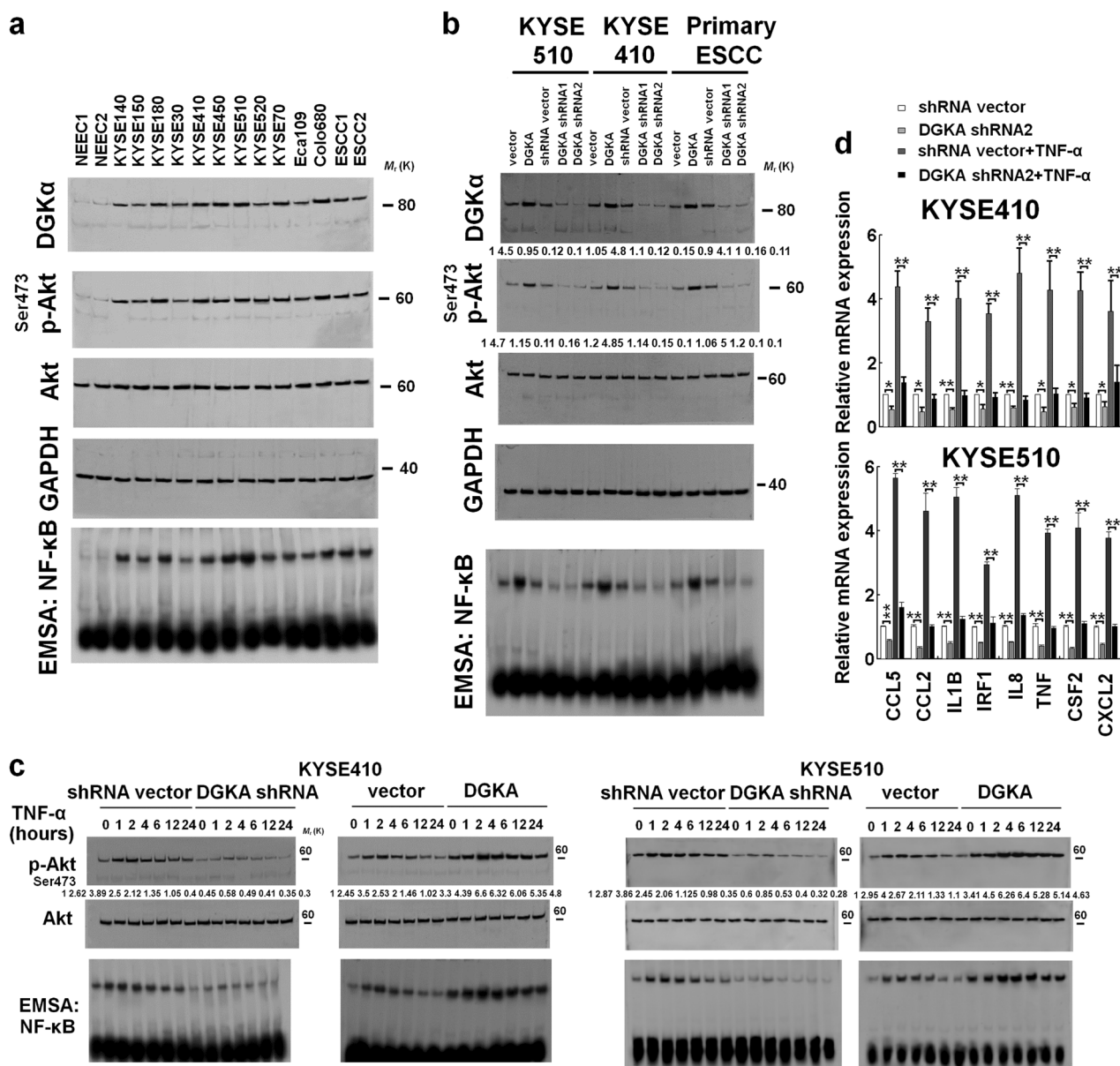


Fig. 2 DGK α positively regulates Akt/NF- κ B signaling. **a** Analysis of DGK α , pAkt or Akt proteins or NF- κ B-DGK α promoter binding ability in primary normal human esophageal epithelial cells (NEECs) and cultured ESCC cell lines, primary human esophageal squamous cell carcinoma cells (ESCCs) by immunoblotting or EMSA assays, respectively. GAPDH was used as a loading control. **b** Immunoblotting or EMSA analysis of DGK α , pAkt, Akt, or NF- κ B-DGKA promoter binding ability in the indicated cells. GAPDH was used as a

loading control. **c** Immunoblotting or EMSA analysis of pAkt/Akt ratio or NF- κ B-DNA-binding ability in the indicated cells treated with TNF- α (10 ng/ml) for various times (0–24 h). Phosphoprotein blots were stripped and reprobed for their total protein counterparts. **d** Expression of NF- κ B-inducible genes, including *CCL5*, *CCL2*, *IL1B*, *IRF1*, *IL8*, *TNF*, *CSF2*, and *CXCL2*, assayed by real-time PCR. Error bars represent mean \pm SD of three independent experiments

decreased TNF- α -induced expression of several NF- κ B target genes in KYSE410 and KYSE510 cells (Fig. 2d). Collectively, combined with that inflammatory cytokines promote DGK α expression via stimulating Akt/NF- κ B signaling, these data comprehensively indicate that DGK α effectively induces Akt/NF- κ B pathway in ESCC cells.

DGK α activates Akt/NF- κ B signaling by interacting with FAK

To understand how DGK α -activated Akt/NF- κ B signaling, we assessed the phosphorylation profiles of various upstream tyrosine kinases using a ‘phospho-activated’ antibody array against 71 unique protein tyrosine kinases (PTKs). DGK α -overexpressed KYSE510 cells had the

◀ **Fig. 3** DGK α activates PI3K signaling by interacting with FAK Tyr397. **a** Immunoblotting analysis of pFAK Tyr397 and FAK in the indicated cells. **b** Three-way co-immunoprecipitation assay revealed that DGK α interacted with FAK and PI3K regulatory subunit-p85 in the indicated cells. **c** Depletion of DGK α did not affect the interaction between FAK and p85 (left panel). Depletion of p85 did not alter the interaction between FAK and DGK α (middle panel). Depletion of FAK impaired the interaction between DGK α and p85 (right panel) in the indicated cells. **d** FERM domain of FAK associates with DGK α . Schematic structure of FAK was shown (top). Whole-cell lysates (WCLs) of HEK293T cells transfected with Flag-FAK, Flag-FERM domain, Flag-FAK catalytic domain, Flag-FAK c-terminal and HA-DGK α were used for immunoprecipitation and immunoblotting, as indicated (left panel). Catalytic domain of DGK α associates with FAK. Schematic structure of DGK α was shown (top). WCLs of HEK293T cells transfected with Flag-DGK α , Flag- δ EF-hand domain of DGK α , Flag-FAK C1 domain, Flag-FAK catalytic domain and HA-FAK were used for immunoprecipitation and immunoblotting, as indicated (right panel). **e** Far-western blotting analysis showing that DGK α specifically interacted with the FERM domain of FAK. Immunoprecipitated HA-FAK and the FERM domain, or HA-FAK (aa356–680) domain were gel purified, transferred to a membrane, and incubated with His-tagged recombinant DGK α , catalytic, or C1 domain of DGK α , then using an antibody specific to the His or the HA tag. **f** Tyr397 phosphorylation status of the immunoprecipitated FAK from HEK293T cells cotransfected with FAK or FAK (aa1–421) and DGK α or DGK α catalytic domain (FAK A17 antibody was used to recognize the FERM domain of FAK). **g** Activation of PI3K by FAK immunoprecipitates. KYSE410 cells transfected with the indicated plasmids, immunoprecipitated with anti-HA antibody, and subjected to the in vitro PI3K assay

with both FAK and p85 using a three-way immunoprecipitation (IP) with indicated antibodies in ESCC cells. Furthermore, we evaluated the physical interaction between DGK α and FAK, or p85. Figure 3c and Supplementary Fig. 4c shows that DGK α knockdown did not affect the interaction between FAK and p85. p85 knockdown did not produce obvious effect on the interaction between DGK α and FAK. FAK knockdown decreased the interaction between DGK α and p85. Above results suggest that DGK α -activated FAK/PI3K pathway might be dependent on FAK.

To determine which region in FAK is important for its interaction with DGK α , we constructed Flag-tagged wild-type (wt) FAK and various domain mutant plasmids and found that FERM domain of FAK interacted with DGK α in HEK293T cells. Figure 3d shows that the catalytic domain of DGK α interacted with FAK. Figure 3e shows that immunoprecipitated wt FAK and the FERM domain of FAK interacted with His-tagged DGK α or the catalytic domain of DGK α protein using far-Western blotting assay, indicating that DGK α directly interacted with the FERM domain of FAK via its catalytic domain (Fig. 3e).

It has been demonstrated that some proteins, such as ezrin or GPCRs, can bind to the FAK FERM domain and activate FAK [26, 28, 29]. Therefore, we tested whether DGK α -FERM interaction can affect the phosphorylation of FAK at Tyr³⁹⁷. As shown in Fig. 3f, DGK α and its catalytic

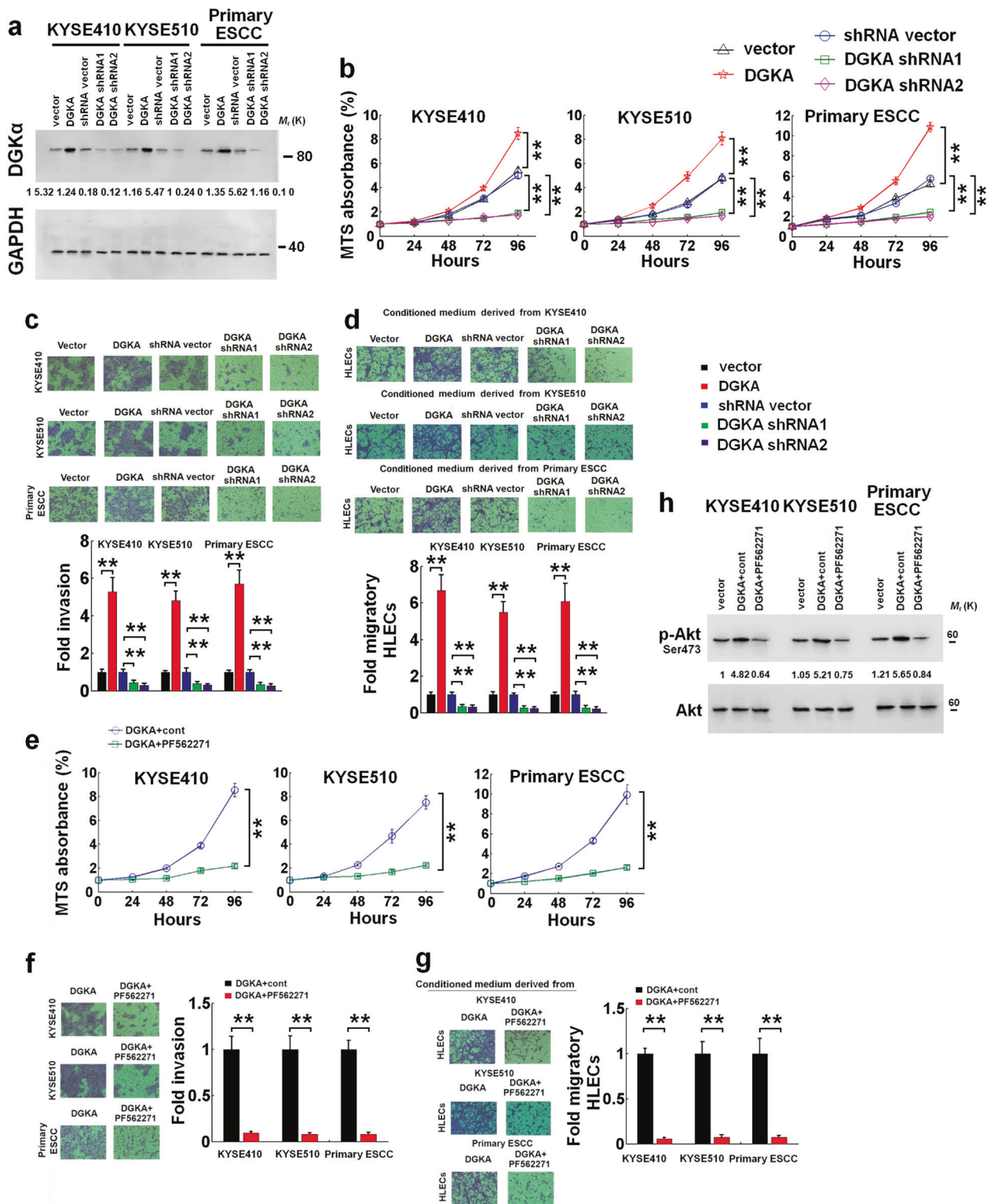
domain effectively induce the phosphorylation of FAK Tyr³⁹⁷ of full-length FAK and FAK truncated mutant (amino acid 1–421). Furthermore, our far-Western blot analysis also revealed that no interaction between DGK α and the site (amino acid 356–680) of FAK (Fig. 3e), excluding the direct phosphorylating effect of DGK α on FAK. Combined with the results that overexpression or depletion of DGK α increased or decreased FAK Tyr³⁹⁷ phosphorylation in ESCC cells (Fig. 3a and Supplementary Fig. 4b), these results together demonstrate that DGK α -FERM interaction can specifically phosphorylate the FAK at Tyr³⁹⁷.

We further examined whether the DGK α /FAK/p85 complex possessed PI3K activity in vitro. The PI3K activity in KYSE410 cells was most significantly stimulated by cotransfection of DGK α and FAK wt plasmids, in the presence of p85 plasmid. Specifically, cotransfection of DGK α and FAK Tyr³⁹⁷ mutant (FAK Y397F) plasmids could not enhance PI3K activity, indicating that wide-type FAK but not FAK Tyr³⁹⁷ mutant is critical for DGK α -mediated PI3K activation (Fig. 3g). Furthermore, cotransfection of DGK α catalytic domain plasmid and FAK wt plasmid, but not FAK Y397F plasmid, in the presence of p85 plasmid could effectively enhance PI3K activity (Fig. 3g). Taken together, these results support the notion that DGK α -mediated activation of FAK/PI3K signaling occurs through the induction of FAK activity via the interaction with FERM domain of FAK.

Expression of DGK α enhances progression of ESCC cells in vitro and in vivo

We examined the oncogenic capacity of DGK α in ESCC cells. Figure 4a, b shows that DGK α stable overexpression enhanced the proliferation of the indicated ESCC cells, while DGK α stable knockdown impaired it. Figure 4c, d shows that DGK α stable overexpression or knockdown markedly increased or decreased the invasion of ESCC cells and their ability to induce the migration of human lymphatic endothelial cells (HLECs). Figure 4e–h shows that the addition of FAK inhibitor-PF562271 significantly offset the effect of DGK α on Akt activation and ESCC malignant progression in vitro.

We further investigated whether DGK α could regulate tumor growth in ESCC in vivo using the subcutaneous xenograft model. Figure 5a shows that DGK α overexpression accelerated the in vivo growth of ESCC tumors, whereas DGK α silence attenuated it. The DGK α -promoted lymphatic metastasis in ESCC was evaluated in vivo using the popliteal lymph node metastasis model. Figure 5b shows that the lymph nodes in tumors formed from DGK α -overexpressed or DGK α -silenced ESCC cells had larger or smaller volumes than those of corresponding control cells.



Next, we examined the effect of DGK α on ESCC metastasis in a lung colonization model. Figure 5c shows that tumor nests in the lungs formed by DGK α -overexpressed or DGK α -depleted ESCC cells had higher or lower numbers than those of their respective parental ESCC cells.

IHC analysis revealed that DGK α -overexpressed or DGK α -depleted ESCC tumors contained increased or decreased lymphatic density, within tumors and their adjacent non-tumor tissue, and proliferative index, within tumors, as indicated by the increased LYVE-1-positive

◀ **Fig. 4** DGK α contributes to ESCC progression in vitro. **a** Immunoblotting analysis of DGK α expression in the indicated cells. GAPDH was used as a loading control. **b** Evaluating the effects of DGK α , DGK α shRNA on the growth of KYSE410 (left), KYSE510 (middle), or primary ESCC cells (right) using MTS assay. **c** Evaluating the effects of DGK α , DGK α shRNA on the invasion of KYSE410 (left), KYSE510 (middle), or primary ESCC cells (right) using Transwell invasion assay. **d** Evaluating the effects of conditioned medium derived from the indicated cells to induce the migration of HLECs using migration assay. **e–h** KYSE410, KYSE510, or primary ESCC DGK α -overexpressing cells were treated with control solvent or 1 μ M FAK functional inhibitor (PF562271). The growth, invasive, or migration ability of HLECs, or Akt activation was evaluated by MTS (**e**), transwell invasion (**f**) or migration assay (**g**), or immunoblotting assay (**h**), respectively. Error bars represent mean \pm SD of three independent experiments. $**P < 0.01$; two-tailed unpaired Student's *t*-test. Error bars represent mean \pm SD of triplicate independent experiments

lymphatic vessels and Ki-67-positive tumor cells, respectively (Supplementary Fig. 5a–c). IHC analysis also showed that DGK α overexpression or depletion resulted in the upregulation or downregulation of pFAK (Tyr³⁹⁷)/pAkt (Ser⁴⁷³)/NF- κ B pathway in ESCC tumors (Supplementary Fig. 6a–d).

Additionally, inhibition of FAK activity in DGK α -overexpressed ESCC tumors suppressed the tumor progression (Fig. 5d–f) and the expression of LYVE-1, Ki-67 (Supplementary Fig. 7a–c), and pFAK (Tyr³⁹⁷)/pAkt (Ser⁴⁷³)/NF- κ B pathway (Supplementary Fig. 8a–d). Collectively, these results indicate that DGK α promotes malignancy of ESCC cells through the activation of FAK/Akt/NF- κ B pathway.

DGK α activates Akt partially through PA

PA can promote tumorigenesis via activating signaling pathways [12, 13, 30]. We then evaluated the effect of PA on DGK α /FAK complex and Akt activation. As shown in Fig. 6a, the DGK α functional inhibitor-R59022, inhibiting PA production, dose-dependently suppressed Akt activation, but had no effect on the formation of DGK α /FAK complex and the FAK activation in ESCC cells. Furthermore, exogenous administration of PA dose-dependently induced the Akt activation, while did not influence the formation of DGK α /FAK complex and the FAK activation in ESCC cells (Fig. 6a). PA partially rescued the Akt activity in the presence of R59022 (Fig. 6a).

It has been demonstrated that PA promotes activity of phosphodiesterases to decrease cAMP and resultantly enhances Akt activation [13, 31]. Furthermore, cAMP can upregulate PTEN activity [32]. Therefore, we hypothesized that DGK α -induced PA diminished cAMP levels and PTEN activity to induce Akt activation in ESCC cells. As shown in Fig. 6b, overexpression or depletion of DGK α increased or decreased the formation of DGK α /FAK complex and

FAK or Akt activation. Overexpression or depletion of DGK α decreased or increased the cAMP levels and PTEN activity (Fig. 6c, d). Furthermore, phosphodiesterase-4D inhibitor, rolipram, increased cAMP level and PTEN activity (Fig. 6c, d), as well as reduced the Akt activation (Fig. 6b). Rolipram produced no effect on the formation of DGK α /FAK complex and FAK activation in ESCC cells. Rolipram blocked the inhibitory effect of DGK α on cAMP level and PTEN activity (Fig. 6c, d), and partially reversed Akt activation in DGK α -overexpressed ESCC cells (Fig. 6b), supporting the hypothesis that DGK α regulates Akt activity (at least partially) via controlling PA production and cAMP activity.

Correspondingly, regulation of PA/cAMP pathway by R59022 or rolipram enhanced the FAK inhibitor-mediated growth-inhibitory effect in ESCC cells or ESCC cells harboring DGK α -overexpressed plasmid (Fig. 6e–g).

The expression of DGK α is upregulated in esophageal carcinomas and positively correlated with tumor grade

Esophageal samples and their paired adjacent normal tissue (22 pairs) were collected to examine the transcriptional expression of those known type I DGKs genes, including DGKA (DGK α), DGKB (DGK β), or DGKG (DGK γ) by real-time PCR. Figure 7a shows that only the DGK α mRNA was significantly upregulated in ESCC, as compared with that of the corresponding adjacent normal tissues. We evaluated the protein level of DGK α in 134 ESCC tumors and their adjacent normal tissues using immunohistochemistry (IHC) assay. Figure 7b and Supplementary Table 2 shows that the higher protein expression of DGK α was detected in 65% of ESCC tissues as compared with that of the corresponding adjacent normal esophageal tissues. Furthermore, DGK α expression was positively associated with tumor grade, tumor or lymph node status of the ESCC patients (Fig. 7b and Supplementary Table 3). Especially, Fig. 7c shows that the expression of DGK α was positively associated with that of pFAK (Tyr³⁹⁷), pAkt (Ser⁴⁷³), or NF- κ B in ESCC tissues. DGK α levels were also correlated with the expression of TNF- α and IL-1 β in clinical ESCC samples (Supplementary Fig. 9a). Supplementary Fig. 9b, c shows that TNF- α (Supplementary Fig. 9b) or IL-1 β (Supplementary Fig. 9c) expression was significantly correlated with various clinical characteristics, including tumor grade, tumor or lymph node status of the ESCC patients ($n = 20$).

Furthermore, the Kaplan–Meier survival analysis indicated that the higher DGK α expression was tightly associated with poorer survival of ESCC patients ($P = 0.0017$; Fig. 7d). ESCC patients were then divided into four groups based on DGK α /pFAK expression levels. The DGK α (high)/pFAK (Tyr³⁹⁷) (high) group, had the shortest overall

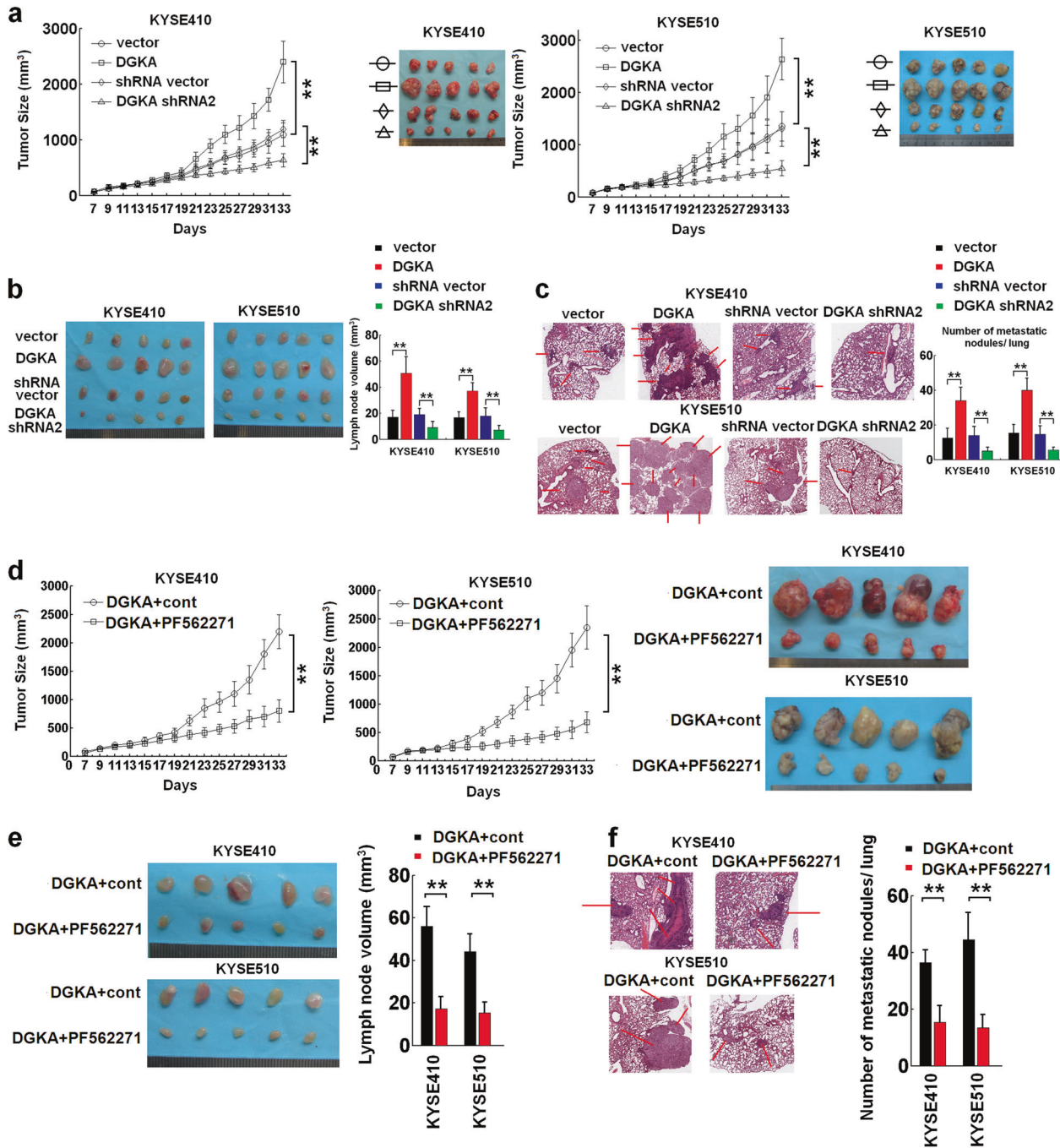
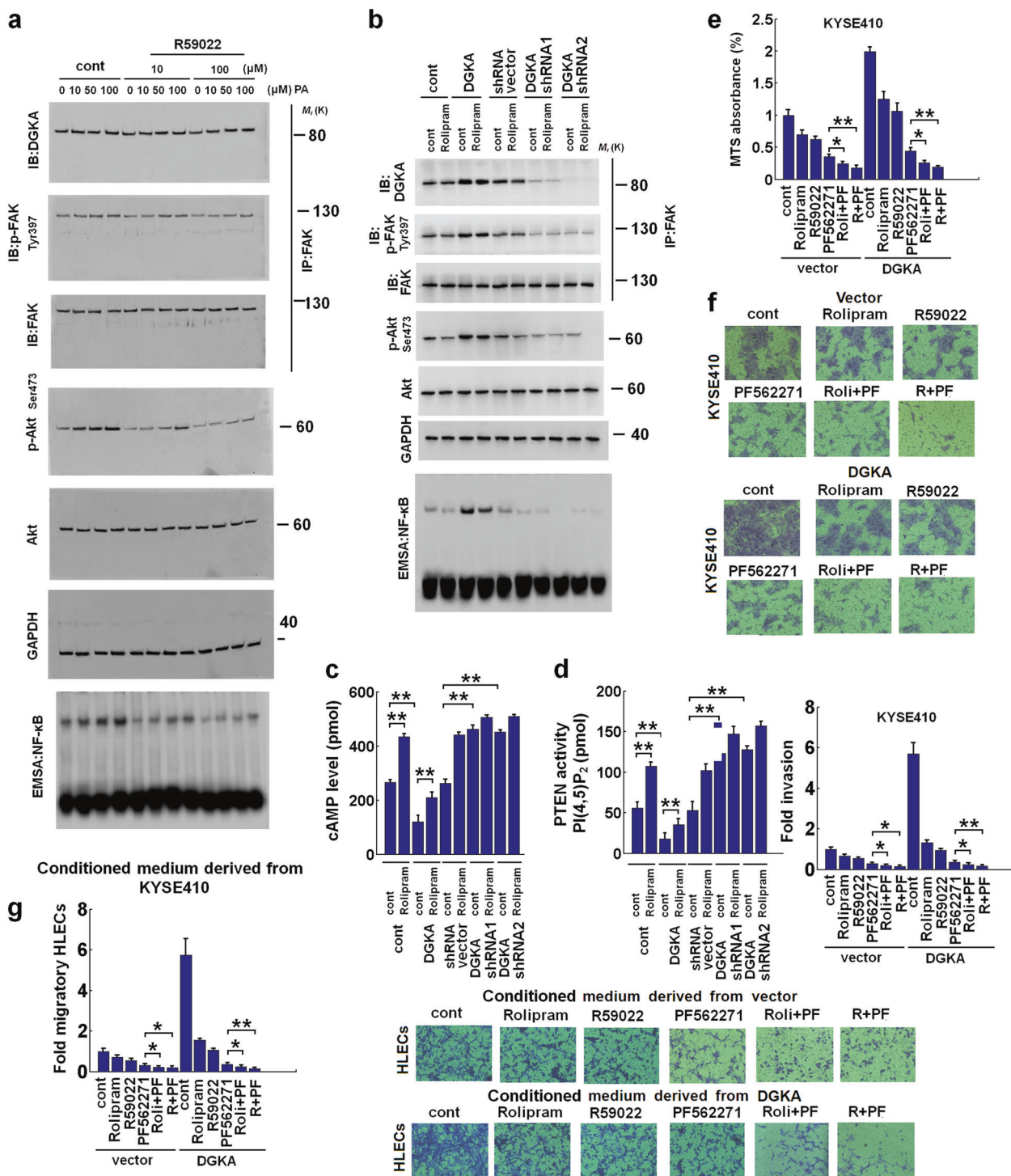


Fig. 5 DGK α contributes to ESCC progression in vivo. **a** KYSE410 and KYSE510 cells stably expressing DGK α or shDGK α or their respective control vector were subcutaneously inoculated into athymic mice ($n = 5$ per group). The growth curves and representative images of tumor were shown. **b** A popliteal lymph node metastasis model was established in athymic mice by inoculating the foot pads with the indicated cells. The popliteal lymph nodes were enucleated and analyzed 5 weeks after inoculation ($n = 5$ per group). Representative images and the volumes of popliteal lymph nodes were shown. **c** A lung colonization model was established in athymic mice by injecting intravenously with the indicated cells via lateral tail veins ($n = 5$ per group). Representative H&E staining of lungs and the number of metastatic nodes on the surface of the lungs were shown. **d** KYSE410 and KYSE510 cells stably expressing DGK α were subcutaneously

inoculated into athymic mice treated with PF562271 (25 mg/kg/day, p. o.) ($n = 5$ per group). The growth curves and representative images of tumor were shown. **e** A popliteal lymph node metastasis model was established in athymic mice by inoculating the foot pads with the indicated cells. The popliteal lymph nodes were enucleated and analyzed 5 weeks after inoculation ($n = 5$ per group). Representative images and the volumes of popliteal lymph nodes were shown. **f** A lung colonization model was established in athymic mice by injecting intravenously with the indicated cells via lateral tail veins ($n = 5$ per group). Representative H&E staining of lungs and the number of metastatic nodes on the surface of the lungs were shown. ** $P < 0.01$; two-tailed unpaired Student's t -test. Error bars represent mean \pm SD of five independent experiments



survival times, compared with other three groups (Fig. 7e). The similar results were also obtained in DGK α /pAkt (Ser⁴⁷³) (Fig. 7f) or DGK α /NF- κ B (Fig. 7g) expression levels. These data are consistent with a role of DGK α in promoting carcinogenesis and support the observation that pFAK (Tyr³⁹⁷)/pAkt (Ser⁴⁷³)/NF- κ B pathway is downstream of DGK α .

Real-time PCR assay was used to evaluate the mRNA expression of DGK α , DGK β , or DGK γ from various squamous carcinomas samples, including lung, cervix, oral, or larynx. The results showed that DGK α was overexpressed in all of these squamous carcinomas while not DGK β or DGK γ (Supplementary Fig. 10a–d). Moreover, the expression of DGK α protein was significantly correlated

◀ **Fig. 6** DGK α activates Akt/NF- κ B pathway partially through phosphatidic acid (PA). **a** KYSE410 cells treated with DMSO, 10 or 100 μ M DGK α functional inhibitor-R59022 with or without the indicated doses of PA for 1 h. Lysates were immunoprecipitated by using anti-FAK antibody and analyzed for coimmunoprecipitating DGK α , FAK, or pFAK antibody using immunoblotting. Akt activity is represented as the levels of phosphorylated forms of Akt compared with total Akt. NF- κ B activity is analyzed by EMSA assay. **b** KYSE410 control cells or their-harbored DGK α or DGK α shRNA plasmids were treated with DMSO or 50 μ M Rolipram for 1 h. Lysates were immunoprecipitated by using anti-FAK antibody and analyzed for coimmunoprecipitating DGK α or pFAK antibody using immunoblotting. Akt activity is represented as the levels of phosphorylated forms of Akt compared with total Akt. NF- κ B activity is analyzed by EMSA assay. **c** The indicated cells were treated with 50 μ M Rolipram for 1 h. Whole cell lysates from the indicated cells were subjected to a direct cAMP ELISA kit. **d** The indicated cells were treated with 50 μ M Rolipram for 1 h. Whole cell lysates from the indicated cells were subjected to immunoprecipitation with antibody against PTEN. The precipitated PTEN was subjected to analysis of PTEN lipid phosphatase activity using a PTEN activity ELISA kit. **e–g** KYSE410 or KYSE410 DGK α -overexpressing cells respectively treated with Rolipram, R59022, PF562271, Rolipram+PF562271 (Roli+PF), or R59022+PF562271 (R+PF). Cell growth was evaluated using MTS assay (**e**). Cell invasion was evaluated using transwell invasion assay (**f**). The cell migration of human lymphatic endothelial cells (HLECs) cultured with conditioned medium derived from the indicated cells was evaluated using migration assay (**g**). * $P < 0.05$; ** $P < 0.01$; two-tailed unpaired Student's t -test. Error bars represent mean \pm SD of triplicate independent experiments

to various clinical parameters (Supplementary Fig. 10e–h, Supplementary Table 2, and Supplementary Tables 4–7) and pFAK (Tyr³⁹⁷)/pAkt (Ser⁴⁷³)/NF- κ B pathway in these types of carcinomas (Supplementary Fig. 11a–d). Taken together, these data support a role for DGK α in promoting progression of squamous carcinomas and suggest that DGK α could serve as a biomarker for cancer diagnosis and a potential target for cancer therapy.

Discussion

Cancer-associated inflammation is often induced by various mediators (cytokines, chemokines, and growth factors) produced by the tumor, stroma, and infiltrating cells. These factors actively promote the malignant progression of cancer cells through activating many important oncogenic signaling pathways, such as PI3K/Akt/NF- κ B and JAKs/STATs pathways. Here, we show that DGK α , upregulated by inflammatory cytokines, stimulates Akt/NF- κ B pathway in a feedforward-loop manner, and promotes ESCC progression and metastasis.

As a major cytokine responsible for activation of Akt/NF- κ B pathway, TNF- α , has been demonstrated to play an important role in promotion of malignant properties in multiple types of cancer [22]. However, TNF- α activates NF- κ B in a relatively short time-course manner in ESCC

cells [7]. In this study, our data show that DGK α can synergize with TNF- α to activate the Akt/NF- κ B pathway, linking the DGK α and cytokine-activated Akt/NF- κ B pathway in ESCC cells. These results suggest that DGK α facilitates the response of Akt/NF- κ B pathway to inflammatory stimulation. Recent advances have highlighted that the aberrant activation of Akt/NF- κ B pathway is widely observed in ESCC, which can induce the expression of several cancer-promoting molecules [7, 33]. This study shows that overactivated Akt/NF- κ B pathway effectively induces the transcriptional expression of DGK α , broadening the role of Akt/NF- κ B pathway in mediating tumorigenesis. We also find that, reciprocally, DGK α is capable of activating Akt/NF- κ B pathway even without exogenous inflammatory stimulation, suggesting that DGK α may be an essential ‘gatekeeper’ of Akt/NF- κ B pathway in ESCC cells.

Due to that activation of PI3K/Akt/NF- κ B pathway is under the control of various tyrosine kinases, such as EGFR, Her3, or FAK [19, 20, 26, 27], we postulate whether DGK α -stimulated PI3K/Akt/NF- κ B pathway may possibly be dependent on the activation of these tyrosine kinases. Our tyrosine kinase antibody array analyses show that DGK α significantly regulates the phosphorylation of FAK at Tyr³⁹⁷, which is a critical signaling transducer in ESCC cells.

For many cytoplasmic tyrosine kinases, intramolecular domain–domain interactions act as another level of negative regulation of their phosphorylation status and preventing aberrant activation of the kinases in response to various activation signals. Interaction of the intramolecular FERM domain of FAK has also been found to open the phosphorylation of FAK at Tyr³⁹⁷ and resultantly create a motif that is recognized by various SH2-domain-containing proteins, especially the p85 subunit of PI3K [26, 27]. David et al. reported that activated-receptor kinases, such as the EGFR and PDGFR can interact with FERM domain of FAK, thus stimulating FAK phosphorylation at Tyr³⁹⁷ [34]. Similar with this observation, our results show that interaction of DGK α with FERM domain of FAK is also critical for the phosphorylation of FAK at Tyr³⁹⁷ and lead to induction of its downstream PI3K/Akt activity. However, our tyrosine kinases antibody array analyses show that DGK α cannot activate EGFR and PDGFR in ESCC cells, indicating that EGFR and PDGFR are not involved in DGK α -stimulated PI3K/Akt signaling in ESCC cells. Importantly, in Fig. 3c IP assays, FAK siRNA does not seemingly induce a loss of DGK α expression in input group. However, in vivo study of Supplementary Fig. 8 shows that PF562271 reduces the protein levels of total DGK α . The possible explanation of this discrepancy may be that as the long-term period of in vivo experiment, FAK inhibitor could sufficiently inhibit the expression of DGK α .

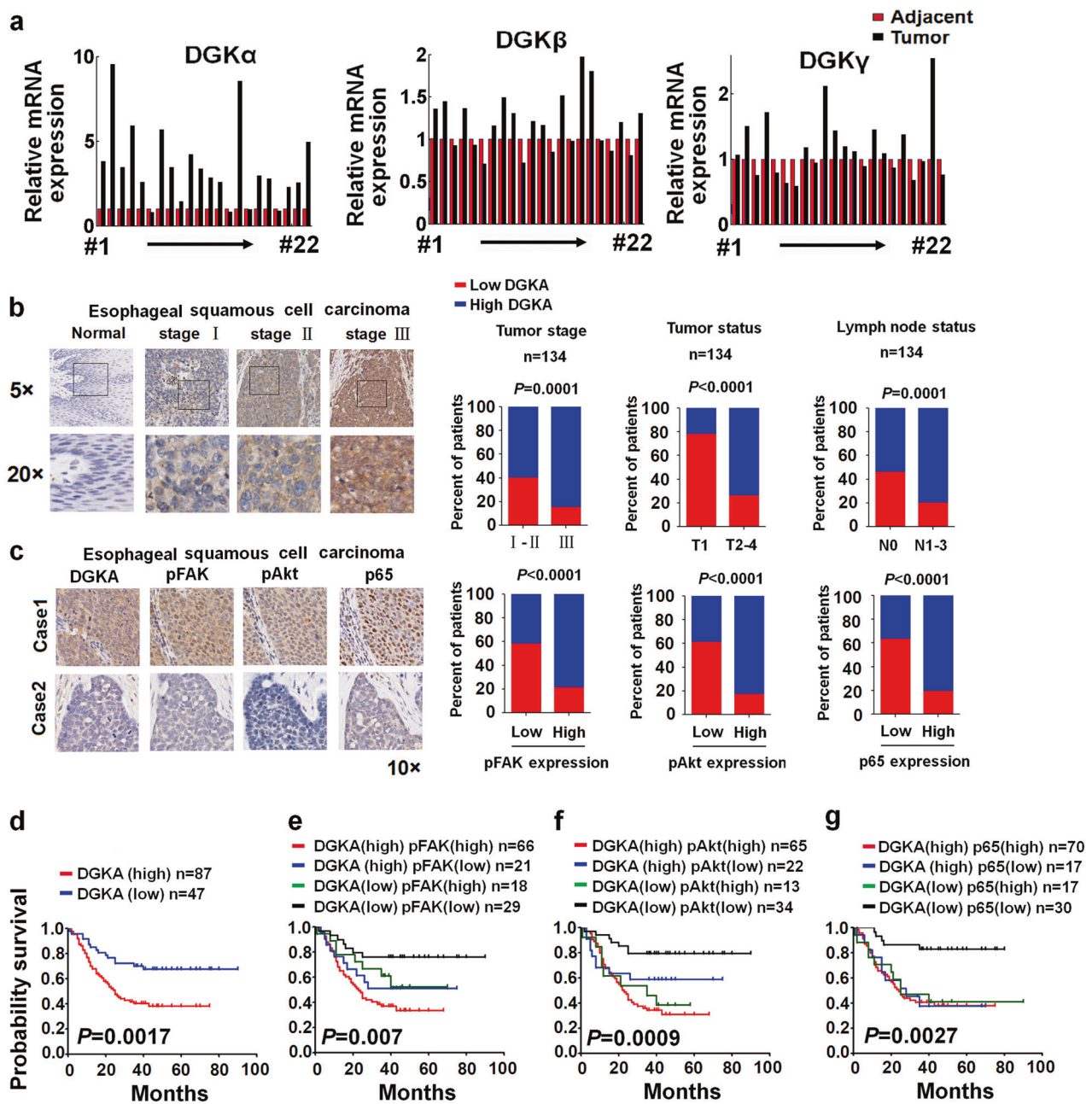


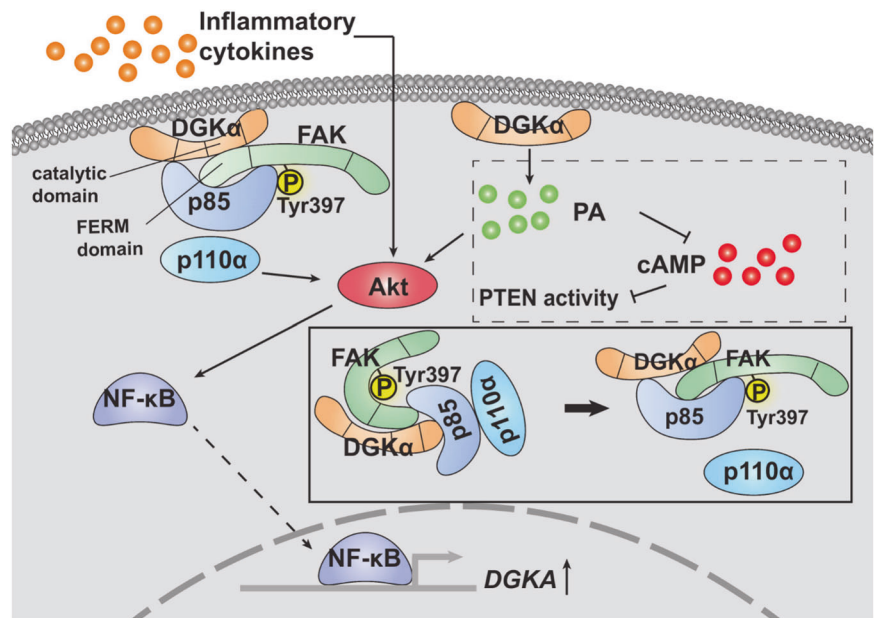
Fig. 7 DGK α positively correlates with the progression of ESCC. **a** Real-time PCR was performed to evaluate the expression level of DGKA (DGK α), DGKB (DGK β), or DGKG (DGK γ) in 22 pairs of ESCC and their corresponding adjacent non-tumorous tissues. Relative levels of DGKA (DGK α), DGKB (DGK β), or DGKG (DGK γ) transcripts were normalized to that of GAPDH and calibrated to the mean mRNA level (arbitrary value of 1) in matched normal tissue. **b** Immunohistochemical staining indicating that DGK α expression in human ESCC (clinical stages I–III) compared with normal esophageal tissue. Magnification, $\times 5$ and $\times 20$ as indicated. Percentages of patients with high expression (SI ≥ 8) of DGKA and low expression (SI < 8) of DGK α according to different clinical parameters as follows: tumor

stage, tumor status and lymph node status ($n = 134$). Two-tailed Pearson χ^2 test. **c** DGK α expression associated with pFAK, pAkt, or NF- κ B expression in 134 primary human ESCC specimens. Two representative specimens with low (SI < 8) and high (SI ≥ 8) levels of DGK α were shown. Magnification, $\times 10$ as indicated. Percentages of specimens showing low (SI < 8) or high (SI ≥ 8) DGK α expression relative to the level of pFAK, pAkt, or NF- κ B. Two-tailed Pearson χ^2 test. **d** Kaplan–Meier curves of ESCC patients with low (SI < 8) vs. high (SI ≥ 8) expression of DGK α ($n = 134$; $P = 0.0017$, log-rank test). **e–g** A Kaplan–Meier analysis of the correlation of DGK α /pFAK (**e**), DGK α /pAkt (**f**), or DGK α /NF- κ B (**g**) coexpression with overall survival

Therefore, these observations point out the importance of DGK α -released the inhibition of FERM domain on FAK phosphorylation at Tyr³⁹⁷ and uncover a novel mechanism

that abrogation of the autonegative regulation of FAK activity in cancer cells.

Fig. 8 Proposed model of feedforward reciprocal activation of DGK α and Akt/NF- κ B signaling regulates ESCC progression DGK α was upregulated by inflammatory stimulants and formed feedforward loop with Akt/NF- κ B signaling. DGK α -activated Akt/NF- κ B signaling via stimulating PA production to reduce cAMP level and PTEN activity, and specifically, independently of its kinase function, through directly interacting with the FERM domain of FAK to relieve the auto-inhibitory effect of FERM domain on FAK to create a binding site for the p85 subunit of PI3K



The present study also finds that the catalytic domain of DGK α specifically contributes to the interaction between DGK α and FERM domain of FAK. Previous studies demonstrated that DGK α produces PA mainly dependent on the activity of its catalytic domain [35]. However, our in vitro results show that DGK α can directly interact with FERM domain of FAK and subsequently induce the phosphorylation of FAK at Tyr397 in the absence of PA. Furthermore, our in vivo data show that exogenous PA or depletion of PA production cannot affect the interaction between DGK α and FAK. These results exclude the possibility that the DGK α -derived PA affects the interaction between DGK α and FAK.

PA contributes to the activation of many intracellular signaling pathways. Especially, Charli L. Domingues et al. reported that DGK α -produced PA can promote activity of phosphodiesterases to decrease cAMP and resultantly enhance the mTOR transcriptional activity in gliomas [13]. Furthermore, intracellular cAMP inhibits Akt activation via enhancing PTEN activity as reported by several groups [32, 36]. In the present study, our data show that DGK α -mediated PA production can suppress the cAMP/PTEN activity and concomitantly enhance the Akt activation. These findings reveal another important mechanism for DGK α -mediated Akt activation that involves PA production. Taken together, the results presented in Fig. 6 demonstrated that DGK α -derived PA can activate Akt pathway and stimulate the progression of ESCC cells. This DGK α /PA-mediate ESCC progression is independent of the formation of DGK α /FAK complex and FAK activation. However, the effect of Rolipram on Akt activation in Fig. 6b is small and some what variable. These results help us comprehensively grasp the function of DGK α .

In summary, our study revealed that DGK α forms feedforward loop with inflammatory cytokines-activated Akt/NF- κ B pathway and promotes ESCC progression. Our mechanistic analyses further showed that DGK α activates Akt/NF- κ B signaling mainly by interacting with FERM domain of FAK, which is independent of its kinase function. Therefore, this study indicates that DGK α functions as a targetable oncogene that links inflammation and tumor progression and strongly supports the pursuit of DGK α as a target for cancer therapy (Fig. 8).

Methods

Reagents

Antibody against DGK α (Cat# H00001606-B01P), TNF- α (Cat# MAB6322), and IL-1 β (Cat# MAB10697) were from Abnova, antibodies against pAkt (Ser473) (Cat# 4060), Akt (Cat# 4691), pFAK (Tyr397) (Cat# 3283S), FAK (Cat# 3285), p85 (Cat# 4292), Ki-67 (Cat# 9027), PTEN (Cat# 9188), GAPDH (Cat# 5174), and Flag (Cat# 2368) were from CST, antibodies against His (Cat# SAB1306084), NF- κ B p65 (Cat# SAB4502615) were Sigma-Aldrich, antibodies against LYVE-1 (Cat# ab14917) were from Abcam. Akt inhibitor (MK2206) (Cat# S1078), FAK inhibitor (PF562271) (Cat# S7357), NF- κ B inhibitor (JSH-23) (Cat# S7351), phosphodiesterase-4D inhibitor (Rolipram) (Cat# S1430) were purchased from Selleck Chemicals, NF- κ B inhibitor (Sc-3060) (Cat# Sc-3060) was from Santa Cruz, phosphatidic acid (PA) (Cat# P9511-10MG) and DGKA inhibitor (R59022) (Cat# D5919-5MG) were from Sigma-Aldrich, TNF- α (Cat# 210-TA-020) and IL-1 β (Cat# 201-

LB-025) were from R&D Systems. FAK (A17) (Cat# sc-557), LPS (Cat# sc-221855A), p85 siRNA (Cat# sc-36217), FAK siRNA (Cat# sc-29310) were from Santa Cruz. All plasmids were from Shanghai Generay Biotechnology Co. Ltd.

Cell lines and transfection

NEECs were obtained from the adjacent noncancerous esophageal tissue and cultured as described previously [37]. KYSE140, KYSE150, KYSE180, KYSE30, KYSE410, KYSE450, KYSE510, KYSE520, KYSE70, Eca109, and Colo680 were generously provided by Dr. Shemada of Kyoto University and cultured as described previously [17]. All cell lines were recently authenticated by the short tandem repeat (STR) method using the AmpF/STR Identifier Kit (Applied Biosystems). HLECs were purchased from Sciencell Research Laboratories (Sciencell, Carlsbad, CA, USA). Primary esophageal squamous cell carcinoma (ESCC) cells were isolated from two cases of freshly removed tumor samples using Cell Isolation Kit (Panomics) according to the manufacturer's instruction. All cells were free of mycoplasma infection.

For stable transfection of DGK α short hairpin RNA (shRNA), KYSE410, KYSE510, and primary ESCC cells were transfected with the pLKO.1 vector (Addgene) and pLKO.1 vector expressing shRNA for DGK α knockdown (pLKO.1-sh DGK α) and were subsequently selected by 0.5 μ g/ml puromycin for 10 days. The DGK α shRNA sequences were as follows: shRNA1-AGACACCTAAGCCTGGCACTGTTTCAATC and shRNA2-GACAGGTGTTCAACCTCCTAAAGGATGGT. For stable transfection of DGK α overexpressing plasmid, pMSCV/DGK α was transfected into KYSE410, KYSE510, and primary ESCC cells, and then cultured for 10 days with 0.5 μ g/ml puromycin after infection. The positive clones were collected for further study.

For other transfection experiments, pcDNA3.1-Flag-FAK, Flag-FAK FERM domain, Flag-FAK catalytic domain, Flag-FAK C terminal domain, or pcDNA3.1-Flag DGKA, Flag-DGKA Δ EF-hand domain, Flag-DGKA C1 domain, Flag-DGKA catalytic domain were transiently cotransfected with pcDNA3.1-HA-DGKA or pcDNA3.1-HA-FAK into HEK293T cells for 48 h. Then, the cell lysates were collected for further study.

Cell proliferation/viability assay

The Cell Titer 96[®] Aqueous One Solution Cell Proliferation Assay (Progenia) was used to evaluate the cell proliferation/viability in the indicated ESCC cells. Briefly, 10 μ l MTS solution was added to each well of the 96-well plate and incubated for 1 h at 37 °C. The absorbance (optical density,

OD) was read at a wavelength of 490 nm for MTS solution on an ELISA plate reader. All experiments were performed in triplicate.

Invasion and migration assay

Invasion of indicated ESCC cells was assessed using 24-well Boyden chambers (Corning, NY) with 8 μ M-inserts coated with Matrigel. The indicated ESCC cells (3×10^4 /well) were plated on the inserts with or without indicated agents for 16 h, the invaded cells that crossed the inserts were stained with 0.1% crystal violet solution, and counted as cells per field of view under phase-contrast microscopy.

For migration assay, the HLECs (2×10^4 /well) were plated on the inserts of 24-well Boyden chambers and incubated with condition medium (CM) from indicated cells in the lower compartment at 37 °C for 24 h. Subsequent experiment was similar with above invasion assay. All experiments were repeated at least three times.

IP and immunoblot analyses

For IP, indicated cells were lysed in IP lysis buffer (ThermoFisher Scientific) supplemented with protease inhibitor and phosphatase inhibitor cocktail (Roche). Cell lysates were incubated on ice for 40 min, and centrifuged at 12,000 \times g at 4 °C for 15 min. The precleared extracts (pre-cleared with protein A/G-agarose beads (ThermoFisher Scientific)) were incubated with the indicated antibodies (5 μ g) for overnight at 4 °C, and then subjected to immunoblot assay.

Immunoblot assay was done as previously described [17]. Briefly, protein extracts were resolved through 8–15% SDS-PAGE, transferred to polyvinylidene fluoride (PVDF) membranes, and incubated with indicated antibodies (All antibodies were diluted at 1:1000; except GAPDH, diluted at 1:3000) for overnight at 4 °C. Following with TBS-T (TBS containing 0.1% Tween-20), the blot was incubated with corresponding peroxidase-labeled secondary antibodies, and the antigen-antibody reaction was visualized by enhanced chemiluminescence (ECL, Pierce) according to manufacturer instructions.

Antibody arrays

For the PTK activation study, human receptor tyrosine kinase phosphorylation antibody array (Raybiotech; catalog AAH-PRTK-1) was used according the manufacturer's instruction. Cell lysates (1 mg) were added to each membrane. Spot quantization was done using a GS-700 Imaging Densitometer (Bio-Rad), with a fixed volume size for all spots being compared, and mean densities were calculated for each spot in duplicate.

Far-western blot analysis

For far-western blot analysis, indicated proteins were immunoprecipitated with HA-tag affinity gel (Sigma-Aldrich), resolved by SDS-PAGE, and then transferred to PVDF membranes, which were subsequently blocked with nonfat dry milk (CST; catalog 9999) for 1 h at 4 °C. His-DGKA protein or its indicated mutants (5 μ g/ml) was respectively incubated with membranes at 4 °C for overnight. Then, the membrane was immunoblotted with anti-His antibody (Sigma-Aldrich). PCR primers for recombinant proteins of DGK α , DGK α catalytic domain, and C1 domain are as follows: pET-28a(+) DGKA, 5'-CCCCAGTGATTTTGCCCA-3' and 5'-GGTTCAAGGCTGGCTTGGA-3'; pET-28a(+) DGKA catalytic domain, 5'-TCTACATCTGAGGCCCTCCG-3' and 5'-CAGACTTTTCCTCTGTCTGCTGAG-3'; pET-28a(+) DGKA C1 domain, 5'-GAGATGACACTGAAGGACGACG-3' and 5'-GAATGTGGTCCCGGAGGAG-3'.

PI3K kinase assay

Cells were transfected with the indicated plasmids. Cell lysates immunoprecipitated with anti-HA antibody were incubated with phosphatidylinositol (substrate) and [γ -³²P] ATP to examine the production of PI (3, 4, 5) P₃ (PIP₃), which was used to evaluate the PI3K activity. Positive control included that recombinant human PI3K p110 α /p85 α protein (Abcam, Cat# ab91093), phosphatidylinositol (substrate) and [γ -³²P] ATP, whereas negative control only included recombinant human PI3K p110 α /p85 α protein. Immunoblotting was used to detect the expression of p85 α followed by IP with HA-antibody and the level of p85 α in recombinant human PI3K protein in positive and negative control groups.

cAMP concentration assay

cAMP activity was measured using a direct cAMP ELISA kit (Biovision; catalog K-371) as previously described [38]. In brief, indicated cells were washed in ice-cold PBS, harvested by centrifugation at 1800 \times g for 5 min and extracted with 0.1 M HCl. The extracts were centrifuged at 15,000 \times g for 3 min and the supernatants were collected. The value of intracellular cAMP levels was read the 96-well plate at OD 450 nm. All experiments were carried out in triplicate.

PTEN lipid phosphatase activity assay

The PTEN lipid phosphatase activity was measured using a PTEN activity ELISA kit (Echelon Biosciences; catalog K-4700) as previously described [39]. Briefly, 30 μ l PTEN

precipitates from the indicated cells were incubated with 30 μ l PI (3, 4, 5) P₃ (16 μ M) substrate at 37 °C for 2 h. The lipid phosphatase activity of PTEN was quantitated by the production of PI (4, 5) P₂. The OD value was read at a wavelength of 450 nm for PI (4, 5) P₂ on an ELISA plate reader. All experiments were carried out in triplicate.

Chromatin immunoprecipitation

ChIP assay was done using SimpleChIP plus enzymatic chromatin IP kit (Cell Signaling Technology; catalog 9004) according to the manufacturer's procedure. Briefly, KYSE410 and KYSE510 cells (1×10^7) were incubated with 1% formaldehyde to crosslink chromatin-associated proteins to DNA. The cells were then sonicated and incubated with 10 μ g NF- κ B p65 or IgG antibody (negative control) per sample. Non-immunoprecipitated chromatin fragments were used as an input control. The primers targeted DGKA promoters were as follows: site 3: forward: 5'-CCCAGGACTGGGAAACTA-3', reverse: 5'-CTGGGATACTGACATCCTAGAGAAA-3', site 2: forward: 5'-AGAAACAGAGACAGAGGACAGACA-3', reverse: 5'-CTTCTCTCCTAGTCCCTCCCTA-3', site 1: forward: 5'-AGCTGGCTCTTCCCCTGTA-3', reverse: 5'-TTCTCAAGGATGGCCAGAAA-3'.

Electrophoretic mobility shift assay

EMSA was conducted using the LightShift Chemiluminescent EMSA kit (Pierce) according to the manufacturer's instruction. The following DNA probes containing specific NF- κ B-DGKA promoter binding sites were used: NF- κ B p65: site 1 (-70 to -60), 5'-CTACCCTCTGAA-GAGGTCCAAGCAAC-3', the final concentration of site 1 probe was 50 fmol, and the final concentration of site 1-specific competitors (100 \times) was 5 pmol. site 1 mutant, 5'-CTACCCTCTGAGGGTCCAAGCAAC-3', the final concentration of site 1 mutant competitors (100 \times) was 5 pmol. site 2 (-126 to -116), 5'-GGACACAGGGAAAGGAA-GATGTTTAGG-3', the final concentration of site 2 probe was 50 fmol, and the final concentration of site 2-specific competitors (100 \times) was 5 pmol. site 2 mutant, 5'-GGACACAGGGAGGAGATGTTTAGG-3', the final concentration of site 2 mutant competitors (100 \times) was 5 pmol. site 3 (-934 to -923), 5'-ATCGTCCCAGGACTGG-GAAACTAGATC-3', the final concentration of site 3 probe was 50 fmol, and the final concentration of site 3-specific competitors (100 \times) was 5 pmol. site 3 mutant, 5'-ATCGTCCCAGCGGGAAACTAGATC-3', the final concentration of site 3 mutant competitors (100 \times) was 5 pmol. Furthermore, the NF- κ B consensus oligo (universal probe) was as follows: 5'-

AGTTGAGGGGACTTCCAGGC-3'. The final concentration of universal probes of NF- κ B was 50 fmol.

Real-time PCR

Real-time PCR was done using $\Delta\sigma$ Ct method to the instructions of the manufacturer on the ABI Prism7000 system (Applied Biosystems). Briefly, total RNA from cells and clinical tissues was extracted with the Trizol reagent (Invitrogen) and then reversely transcribed into first-strand cDNA using Superscript First-Strand cDNA Synthesis kit (Invitrogen). The human *GAPDH* gene was used as an internal standard. The experiment was repeated three times. Primers are as follows: *DGKA*, 5'-TGAGTCCCTAGGCCCTCCATC-3' and 5'-CCCTGGCCAAAAGTAGGGAG-3'; *DGKB*, 5'-CCTATCAGGCGGTCTGAGAAT-3' and 5'-GGAA-CACGTATTTGCAGGAGAAG-3'; *DGKG*, 5'-GACCCACATGAGCCGATTAGC-3' and 5'-GTGGTCA-GAGGTCTCGTGTCT-3'; *CCL5*, 5'-CCAG-CAGTCGTCTTTGTAC-3' and 5'-CTCTGGGTTGGCACACACTT-3'; *CCL2*, 5'-CAGCCA-GATGCAATCAATGCC-3' and 5'-TGGAATCCT-GAACCCTTCT-3'; *IL1B*, 5'-AGCTACGAATCTCCGACCAC-3' and 5'-CGTTATCC-CATGTGTCGAAGAA-3'; *IRF1*, 5'-ATGCCCAT-CACTCGGATGC-3' and 5'-CCCTGCTTTGTATCGGCCTG-3'; *IL8*, 5'-TTTTGCCAAGGAGTGCTAAAGA-3' and 5'-AACCCTCTGCACCCAGTTTTTC-3'; *TNF*, 5'-CCTCTCTCTAATCAGCCCTCTG-3' and 5'-GAG-GACCTGGGAGTAGATGAG-3'; *CSF2*, 5'-TCCTGAACCTGAGTAGAGACAC-3' and 5'-TGCTGCTTGTAGTGGCTGG-3'; *CXCL2*, 5'-CTCCTTGCCAGCTCTCCTC-3' and 5'-GGGGACTT-CACCTTCACACT-3'; *GAPDH*, 5'-GGAGCGA-GATCCCTCCAAAAT-3' and 5'-GGCTGTTGTCATACTTCTCATGG-3'.

Microarray analysis

Microarray assay was conducted using NimbleGen whole Human Genome 12 \times 135K arrays. The hybridized arrays were scanned with the Axon GenePix 4000B microarray scanner, and the images were then analyzed using the NimbleScan software (version 2.5). All gene level files were imported into Agilent GeneSpring GX software (version 11.5.1). Microarray data were deposited at the Gene Expression Omnibus database with an accession number GSE104768.

Patient information, tissue specimens, and IHC

Tissue specimens used in the present study were collected from ESCC, nasopharyngeal squamous cell carcinoma, oral squamous cell carcinoma, lung squamous cell carcinoma, and cervical cancer (squamous cell carcinoma) patients. The use of human subject was approved from the institutional Review Board of the Cancer institute and Hospital of Chinese Academy of Medical Sciences (CAMS) and Peking University Cancer Hospital and Institute. The exact information of clinical tissue samples used in IHC (including: clinical stage, TMN classification, age and gender) is listed in Tables S2–S7. For IHC assay, the experiment was done according to our previous study [17]. The primary antibodies were diluted at 1:500, except TNF- α and IL-1 β antibodies were diluted at 1:100. Evaluation for immunostaining degree of clinical samples was based on the proportion of positively stained tumor cells and the intensity of staining. The staining index (SI) was calculated as staining intensity score \times proportion of positive tumor cells as described previously [40]. According to this method of assessment, we evaluated the indicated protein expression by determining the SI value, scored as 0, 2, 3, 4, 6, 8, 9, 12, and 16. Protein expression with a SI \geq 8 were determined as high expression and samples with a SI $<$ 8 were determined as low expression.

Animal experiments

For evaluating DGK α -mediated tumor growth, female nu/nu mice (5-week old; Vital River Laboratory animal technology Co., Ltd) were subcutaneously inoculated with the indicated ESCC cells (5×10^6) into the right flank of animals. All the animals were randomly grouped for experiments ($n = 5$ per group). Tumor sizes were measured every 2 days using a digital caliper, and calculated using the formula: (mm^3) = lengths (L) \times widths (W^2) \times 0.5.

The in vivo lung colonization model was evaluated by intravenously injecting indicated ESCC cells (1×10^6) into the tail vein of nu/nu mice ($n = 5$ per group). The lung was removed and the number of metastatic nodes on the lung surface was calculated after 8 weeks. The exact experiment was conducted according to our previous study [40].

The in vivo popliteal lymph node metastasis model was established with nu/nu mice, which were inoculated with indicated ESCC cell (1×10^6 , $n = 5$ per group) into the foot pads. Lymph node sizes were evaluated by the formula: (mm^3) = ($L \times W^2$) \times 0.5. The exact protocol was according to previous study [41]. All animal work was conducted in accordance with a protocol approved by the Animal Center, PUMC and CAMS, and Peking University Cancer Hospital & Institute.

Statistical analysis

Statistical analyses were performed using the MATLAB7.0 software and Graphpad 5.0 software. Unpaired Student's *t*-test (two-tailed) was used to compare statistical significance between two groups. Chi-square test was used to compare indicated proteins between cancer and adjacent normal tissue, or various clinical parameters. All experiments for cell cultures were conducted independently at least three times. Error bars represent mean \pm SD. In all cases, *P*-value of <0.05 was considered statistically significant. Before statistical analysis, variations within each group and the assumption of the tests were checked.

Acknowledgements This work is supported by the National 973 Program (2015CB553904) and National Natural Fund of China (81830086, 81490753, 81502110, and 81772504). Beijing Municipal Administration of Hospitals's Youth Program, code: QML20171105.

Compliance with ethical standards

Conflict of interest The authors declare that they have no conflict of interest.

References

- Luzzato L, Pandolfi PP. Causality and chance in the development of cancer. *N Engl J Med.* 2015;373:84–88.
- Czechlinska M, Kowalewska M, Nowak R. Systemic inflammation as a confounding factor in cancer biomarker discovery and validation. *Nat Rev Cancer.* 2010;10:2–3.
- Jemal A, Siegel R, Xu J, Ward E. Cancer statistics, 2010. *CA Cancer J Clin.* 2010;60:277–300.
- Elinav E, Nowarski R, Thaiss CA, Hu B, Jin C, Flavell RA. Inflammation-induced cancer: crosstalk between tumours, immune cells and microorganisms. *Nat Rev Cancer.* 2013;13:759–71.
- Wang F, Arun P, Friedman J, Chen Z, Van Waes C. Current and potential inflammation targeted therapies in head and neck cancer. *Curr Opin Pharmacol.* 2009;9:389–95.
- Li Y, Li J, Luo M, Zhou C, Shi X, Yang W, et al. Novel non-coding RNA NMR promotes tumor progression via NSUN2 and BPTF in esophageal squamous cell carcinoma. *Cancer Lett.* 2018;430:57–66.
- Song L, Gong H, Lin C, Wang C, Liu L, Wu J, et al. Flotillin-1 promotes tumor necrosis factor- α receptor signaling and activation of NF- κ B in esophageal squamous cell carcinoma cells. *Gastroenterology.* 2012;143:995–1005. e1012
- Merida I, Avila-Flores A, Merino E. Diacylglycerol kinases: at the hub of cell signalling. *Biochem J.* 2008;409:1–18.
- Martinez K, Shyamasundar S, Kennedy A, Chuang CC, Marsh A, Kincaid J, et al. Diacylglycerol kinase inhibitor R59022 attenuates conjugated linoleic acid-mediated inflammation in human adipocytes. *J Lipid Res.* 2013;54:662–70.
- Okada M, Hozumi Y, Iwazaki K, Misaki K, Yanagida M, Araki Y, et al. DGK ζ is involved in LPS-activated phagocytosis through IQGAP1/Rac1 pathway. *Biochem Biophys Res Commun.* 2012;420:479–84.
- Takeishi K, Taketomi A, Shirabe K, Toshima T, Motomura T, Ikegai T, et al. Diacylglycerol kinase α enhances hepatocellular carcinoma progression by activation of Ras-Raf-MEK-ERK pathway. *J Hepatol.* 2012;57:77–83.
- Torres-Ayuso P, Daza-Martin M, Martin-Perez J, Avila-Flores A, Merida I. Diacylglycerol kinase α promotes 3D cancer cell growth and limits drug sensitivity through functional interaction with Src. *Oncotarget.* 2014;5:9710–26.
- Dominguez CL, Floyd DH, Xiao A, Mullins GR, Kefas BA, Xin W, et al. Diacylglycerol kinase α is a critical signaling node and novel therapeutic target in glioblastoma and other cancers. *Cancer Discov.* 2013;3:782–97.
- Dan HC, Cooper MJ, Cogswell PC, Duncan JA, Ting JP, Baldwin AS. Akt-dependent regulation of NF- κ B is controlled by mTOR and Raptor in association with IKK. *Genes Dev.* 2008;22:1490–1500.
- Wu DW, Lee MC, Hsu NY, Wu TC, Wu JY, Wang YC, et al. FHT1 loss confers cisplatin resistance in lung cancer via the AKT/NF- κ B/Slug-mediated PUMA reduction. *Oncogene.* 2015;34:3882–3.
- Vivanco I, Sawyers CL. The phosphatidylinositol 3-Kinase AKT pathway in human cancer. *Nat Rev Cancer.* 2002;2:489–501.
- Chen J, Lan T, Zhang W, Dong L, Kang N, Zhang S, et al. Platelet-activating factor receptor-mediated PI3K/AKT activation contributes to the malignant development of esophageal squamous cell carcinoma. *Oncogene.* 2015;34:5114–27.
- Castellano E, Sheridan C, Thin MZ, Nye E, Spencer-Dene B, Diefenbacher ME, et al. Requirement for interaction of PI3-kinase p110 α with RAS in lung tumor maintenance. *Cancer Cell.* 2013;24:617–30.
- Hu P, Margolis B, Skolnik EY, Lammers R, Ullrich A, Schlessinger J. Interaction of phosphatidylinositol 3-kinase-associated p85 with epidermal growth factor and platelet-derived growth factor receptors. *Mol Cell Biol.* 1992;12:981–90.
- Hellyer NJ, Cheng K, Koland JG. ErbB3 (HER3) interaction with the p85 regulatory subunit of phosphoinositide 3-kinase. *Biochem J.* 1998;333:757–63.
- Zhou H, Liu W, Su Y, Wei Z, Liu J, Kolluri SK, et al. NSAID sulindac and its analog bind RXR α and inhibit RXR α -dependent AKT signaling. *Cancer Cell.* 2010;17:560–73.
- Balkwill F. TNF- α in promotion and progression of cancer. *Cancer Metastasis-Rev.* 2006;25:409–16.
- Voronov E, Shouval DS, Krelin Y, Cagnano E, Benharroch D, Iwakura Y, et al. IL-1 is required for tumor invasiveness and angiogenesis. *Proc Natl Acad Sci USA.* 2003;100:2645–50.
- Chen MF, Lu MS, Chen PT, Chen WC, Lin PY, Lee KD. Role of interleukin 1 beta in esophageal squamous cell carcinoma. *J Mol Med.* 2012;90:89–100.
- Guo W, Wang N, Li Y, Zhang JH. Polymorphisms in tumor necrosis factor genes and susceptibility to esophageal squamous cell carcinoma and gastric cardiac adenocarcinoma in a population of high incidence region of North China. *Chin Med J.* 2005;118:1870–8.
- Mitra SK, Hanson DA, Schlaepfer DD. Focal adhesion kinase: in command and control of cell motility. *Nat Rev Mol Cell Biol.* 2005;6:56–68.
- Xia H, Nho RS, Kahm J, Kleidon J, Henke CA. Focal adhesion kinase is upstream of phosphatidylinositol 3-kinase/Akt in regulating fibroblast survival in response to contraction of type I collagen matrices via a beta 1 integrin viability signaling pathway. *J Biol Chem.* 2004;279:33024–34.
- Pouillet P, Gautreau A, Kadare G, Girault JA, Louvard D, Arpin M. Ezrin interacts with focal adhesion kinase and induces its activation independently of cell-matrix adhesion. *J Biol Chem.* 2001;276:37686–91.
- Streblov DN, Vomaske J, Smith P, Melnychuk R, Hall L, Pancheva D, et al. Human cytomegalovirus chemokine receptor

- US28-induced smooth muscle cell migration is mediated by focal adhesion kinase and Src. *J Biol Chem.* 2003;278:50456–65.
30. Rainero E, Caswell PT, Muller PA, Grindlay J, McCaffrey MW, Zhang Q, et al. Diacylglycerol kinase α controls RCP-dependent integrin trafficking to promote invasive migration. *J Cell Biol.* 2012;196:277–95.
 31. Nemoz G, Sette C, Conti M. Selective activation of rolipram-sensitive, cAMP-specific phosphodiesterase isoforms by phosphatidic acid. *Mol Pharmacol.* 1997;51:242–9.
 32. Sugimoto N, Miwa S, Ohno-Shosaku T, Tsuchiya H, Hitomi Y, Nakamura H, et al. Activation of tumor suppressor protein PTEN and induction of apoptosis are involved in cAMP-mediated inhibition of cell number in B92 glial cells. *Neurosci Lett.* 2011;497:55–59.
 33. Lin C, Song L, Gong H, Liu A, Lin X, Wu J, et al. Nkx2-8 downregulation promotes angiogenesis and activates NF- κ B in esophageal cancer. *Cancer Res.* 2013;73:3638–48.
 34. Sieg DJ, Hauck CR, Ilic D, Klingbeil CK, Schaefer E, Damsky CH, et al. FAK integrates growth-factor and integrin signals to promote cell migration. *Nat Cell Biol.* 2000;2:249–56.
 35. van Blitterswijk WJ, Houssa B. Properties and functions of diacylglycerol kinases. *Cell Signal.* 2000;12:595–605.
 36. Lou L, Urbani J, Ribeiro-Neto F, Altschuler DL. cAMP inhibition of Akt is mediated by activated and phosphorylated Rap1b. *J Biol Chem.* 2002;277:32799–806.
 37. Andl CD, Mizushima T, Nakagawa H, Oyama K, Harada H, Chruma K, et al. Epidermal growth factor receptor mediates increased cell proliferation, migration, and aggregation in esophageal keratinocytes in vitro and in vivo. *J Biol Chem.* 2003;278:1824–30.
 38. Zhang B, Sun N, Mu X, Zhi L, Zhai L, Jiang Y, et al. G protein alpha S subunit promotes cell proliferation of renal cell carcinoma with involvement of protein kinase A signaling. *DNA Cell Biol.* 2017;36:237–42.
 39. Guo ST, Chi MN, Yang RH, Guo XY, Zan LK, Wang CY, et al. INPP4B is an oncogenic regulator in human colon cancer. *Oncogene.* 2016;35:3049–61.
 40. Chen J, Lan T, Zhang W, Dong L, Kang N, Zhang S, et al. Feed-forward reciprocal activation of PAFR and Stat3 regulates epithelial-mesenchymal transition in non-small cell lung cancer. *Cancer Res.* 2015;75:4198–210.
 41. Ito T, Shimada Y, Kan T, David S, Cheng Y, Mori Y, et al. Pituitary tumor-transforming 1 increases cell motility and promotes lymph node metastasis in esophageal squamous cell carcinoma. *Cancer Res.* 2008;68:3214–24.